Microstrip Lines for Microwave Integrated Circuits

By M. V. SCHNEIDER

(Manuscript received December 2, 1968)

Microstrips, transmission lines of metallic layers deposited on a dielectric substrate, are very useful for the microwave and millimeter wave hybrid integrated circuits required for solid-state radio systems because of their simplicity and planar structure. To design hybrid integrated circuits with microstrips requires computation or measurement of the impedance, the attenuation, the guide wavelength, and the unloaded Q of the line. These parameters can be obtained from the effective dielectric constant and the characteristic impedance of the corresponding air line. This paper gives the exact design data for all line parameters for the most important cases.

We report the impedance and attenuation measurements performed on microstrips. Satisfactory agreement is obtained with theoretical results based on conformal mapping with logarithmic derivatives of theta functions and expressions involving the partial derivatives of the impedance with respect to independent line parameters.

I. INTRODUCTION

Transmission lines and passive lumped or distributed circuit elements, which are manufactured and assembled from planar metal conductors or conducting stripes on insulating substrates, are essential basic elements in microwave and millimeter wave hybrid integrated circuits. The metal strips or microstrips are deposited by thin-film or thick-film technology on dielectric substrates; the processing steps are substantially different compared to conventional coaxial and waveguide circuit technology. Circuits built with microstrip transmission lines or microstrip components have three important advantages:

(*i*) The complete conductor pattern can be deposited and processed on a single dielectric substrate which is supported by a single metal

ground plane. Such a circuit can be fabricated at a substantially lower cost than waveguide or coaxial circuit configurations.

(*ii*) Beam-leaded active and passive devices can be bonded directly to metal stripes on the dielectric substrate.

(*iii*) Devices and components incorporated into hybrid integrated circuits are accessible for probing and circuit measurements (with some limitations imposed by external shielding requirements).

The purpose of this paper is to derive formulas for the electric parameters which are the impedance, attenuation, propagation constant, and unloaded Q of the microstrip transmission line. In addition to the electrical design data, attenuation measurements at 30 GHz are presented because:

(*i*) The attenuation is the most important electrical parameter of a microstrip because it determines the circuit losses of microwave and millimeter wave hybrid integrated circuits.

(*ii*) There are many solid-state radio systems for which hybrid integration looks attractive, such as the radio pole line, high-capacity domestic-satellite systems, *Picturephone*® visual telephone distribution, and mobile telephone systems.[1,2] Hybrid integration of circuits is essential for many other applications in order to achieve small overall size, minimum weight, and low production cost.

II. DEFINITION AND CLASSIFICATION

A strip line or microstrip line is a parallel two-conductor line made of at least one flat strip of small thickness. For mechanical stability the strip is deposited on a dielectric substrate which is usually supported by a metal ground plane. This basic configuration is shown in Fig. 1a.

A parallel two-conductor line of this type may need modification because:

(*i*) A radio frequency shield may be required to eliminate radiation losses. The shield dimensions or the sheet conductivity of the shielding material have to be chosen in such a way that excitation of transverse electric modes, transverse magnetic modes, and box resonances is suppressed.

(*ii*) Proximity of the air-dielectric interface with the strip conductor can lead to excitation of plane-trapped surface waves. This problem can be solved by using a substrate with a low dielectric constant or by choosing a sufficiently small frequency-thickness product

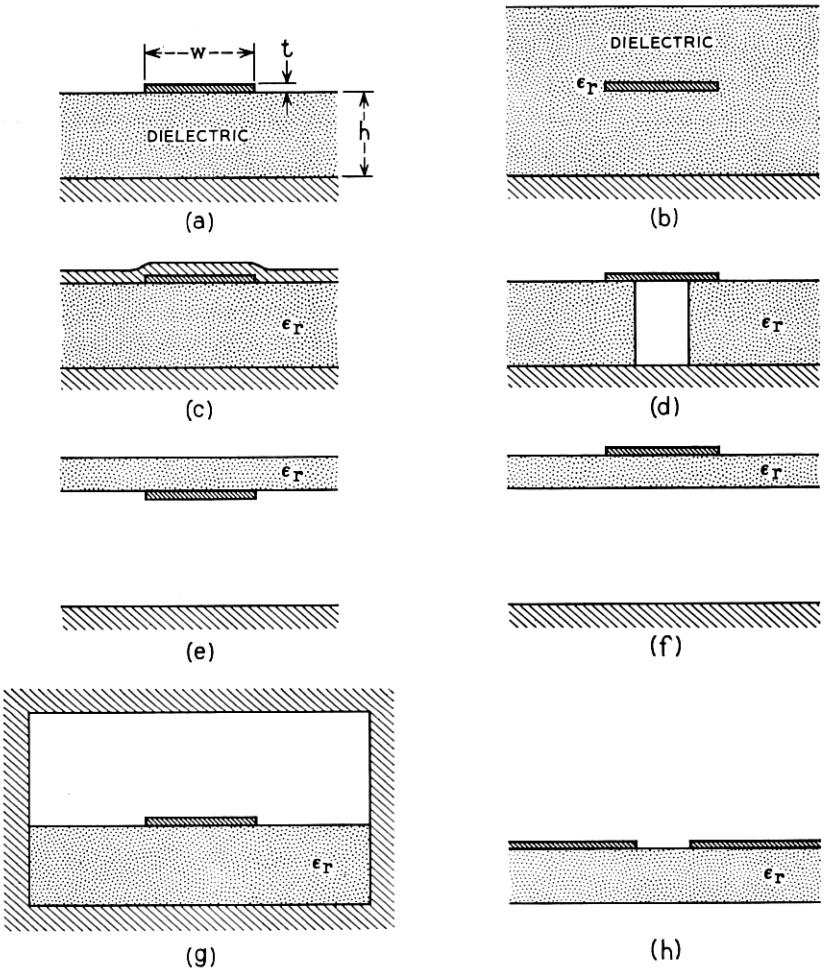

Fig. 1 — Basic types of microstrip transmission lines with one strip conductor supported by a dielectric substrate: (a) standard microstrip, (b) embedded microstrip, (c) microstrip with overlay, (d) microstrip with hole, (e) standard inverted microstrip, (f) suspended microstrip, (g) shielded microstrip, (h) slot transmission line.

for the microstrip. It can also be solved by removing the air-dielectric interface into the far field region as shown in Fig. 1b.

(*iii*) If the substrate is a semiconductor, surface passivation may be necessary to protect against atmospheric contaminants. This can be achieved by a thin dielectric film as shown in Fig. 1c.

(*iv*) Solid-state devices with substantial heat dissipation such as IMPATT, GUNN, and LSA diodes as well as high-power varactor diodes have to be shunt mounted in the microstrip in order to achieve a small thermal spreading resistance in the ground plane. A hole in the dielectric is required in Fig. 1d for mounting a solid state device between the two microstrip conductors.

IMPATT diodes, bulk sources, and high-power varactors are typical examples of solid-state devices which are usually shunt mounted in transmission line circuits. Other solid-state devices or materials which require shunt mounting are ferrites for circulators and isolators and high-Q dielectric resonators for microwave band-pass filters. Shunt mounting is facilitated in inverted microstrips and suspended microstrips shown in Figs. 1e and 1f. Solid-state devices which require a dc bias or a dc return have to be mounted by means of a pressure contact or bonded contacts between the ground plane and the strip conductor shown in Fig. 1e. Complete shielding of such a line is essential because fringe field effects are enhanced by increased electric field intensities in the dielectric support material. An attractive solution is to suspend the substrate symmetrically between the ground plane and the top shield. Such lines have been discussed by Brenner and have been used for balanced transistor amplifiers and ferrite circulators.[3–6] A major advantage of all microstrip configurations with an air gap is that the effective dielectric constant is small. This means that the effective dielectric loss tangent is substantially reduced; also, all circuit dimensions can be increased, which leads to less stringent mechanical tolerances, better circuit reproducibility, and therefore lower production cost.

Figure 1g shows a completely shielded standard microstrip and Fig. 1h is a schematic diagram of a slot line which consists of two conductors deposited on the same side of a high permittivity substrate.[7] The slot line can be tightly coupled to the lines of Figs. 1a through g by depositing the slot line metallization on one side of the substrate and the microstrip conductor on the opposite side of the same substrate. Standard microstrips supporting transverse electromagnetic modes and structures supporting slot modes can thus be combined on one single substrate for obtaining the widest possible choice of circuits to be built with existing hybrid integrated circuit technology.

III. IMPEDANCE, ATTENUATION, AND UNLOADED Q

The electrical parameters of the microstrips of Figs. 1a through g which are required for circuit design are impedance, attenuation, unloaded Q, wavelength, and propagation constant. These parameters are interrelated for all microstrips of Figs. 1a through g assuming that

(*i*) The propagating mode is a transverse electromagnetic mode, or it can be approximated by a transverse electromagnetic mode.
(*ii*) Conductor losses in the metal strips are predominant, which means dielectric losses can be neglected.
(*iii*) The relative magnetic permeability of the substrate material is $\mu_r = 1$.

The basic reason for the subsequently explained relationship of the line parameters is that the inductance per unit length depends only upon the conductor geometry and is absolutely independent of the geometry and the dielectric properties of the supporting structure. The relationship between line parameters is shown in Fig. 2.

Let us assume in Fig. 2a that the conductor geometry is defined by a stripe width w_o, a ground plane spacing h_o, and a small stripe thickness t_o. Let us also assume that this is an air line with a characteristic impedance Z_o, a wavelength λ_o, an attenuation per unit length α_o, and an unloaded Q_o. If the conductor dimensions remain the same, and if the microstrip is fully embedded in a dielectric medium with a relative dielectric constant ϵ_r, one obtains the new line parameters given in Fig. 2b. If the line is only partially filled with dielectric support material with a relative dielectric constant ϵ_r, one obtains for the line parameters of Fig. 2c

$$Z = \frac{Z_o}{(\epsilon_{eff})^{\frac{1}{2}}} \qquad \text{impedance} \tag{1}$$

$$\lambda = \frac{\lambda_o}{(\epsilon_{eff})^{\frac{1}{2}}} \qquad \text{wavelength} \tag{2}$$

$$\alpha = (\epsilon_{eff})^{\frac{1}{2}}\alpha_o \qquad \text{attenuation} \tag{3}$$

$$Q = Q_o = \frac{20\pi}{\ln 10}\frac{1}{\alpha_o\lambda_o} \qquad \alpha_o\lambda_o \text{ in dB.} \tag{4}$$

The effective dielectric constant ϵ_{eff} has to be computed or measured

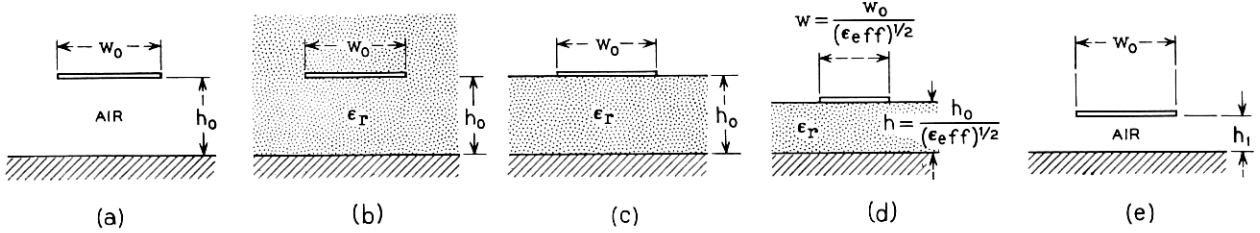

Z_0 IMPEDANCE	$\frac{Z_0}{(\epsilon_r)^{1/2}}$	$\frac{Z_0}{(\epsilon_{eff})^{1/2}}$	$\frac{Z_0}{(\epsilon_{eff})^{1/2}}$	$\frac{Z_0}{(\epsilon_{eff})^{1/2}}$
λ_0 WAVELENGTH	$\lambda = \frac{\lambda_0}{(\epsilon_r)^{1/2}}$	$\lambda = \frac{\lambda_0}{(\epsilon_{eff})^{1/2}}$	$\lambda = \frac{\lambda_0}{(\epsilon_{eff})^{1/2}}$	$\lambda = \lambda_0$
α_0 ATTENUATION	$\alpha = (\epsilon_r)^{1/2}\,\alpha_0$	$\alpha = (\epsilon_{eff})^{1/2}\,\alpha_0$	$\alpha = \epsilon_{eff} \cdot \alpha_0$	$\alpha = (\epsilon_{eff})^{1/2}\,\alpha_0$
$Q_0 = \frac{20\pi}{\ell n\, 10}\,\frac{1}{\alpha_0 \lambda_0}$	$Q = Q_0$	$Q = Q_0$	$Q = \frac{Q_0}{(\epsilon_{eff})^{1/2}}$	$Q = \frac{Q_0}{(\epsilon_{eff})^{1/2}}$

Fig. 2 — Impedance, wavelength, attenuation, and unloaded Q of microstrip transmission lines.

as discussed in Section 4.3. The following inequalities are valid for the standard microstrip in Fig. 1a and the inverted microstrip of Fig. 1e

$$\frac{1+\epsilon_r}{2} \leqq \epsilon_{eff} \leqq \epsilon_r \qquad \text{standard microstrip} \tag{5}$$

$$1 \leqq \epsilon_{eff} \leqq \frac{1+\epsilon_r}{2} \qquad \text{inverted microstrip.} \tag{6}$$

If one has to compare the attenuation or the unloaded Q of different microstrips one has to consider lines which have the same impedance level. It is also necessary that the electrical length of both or at least one critical conductor dimension w or h of Fig. 2 is the same. By critical conductor dimension we mean the dimension which is more critical with respect to excitation of transverse electric modes or transverse magnetic modes. Plane-trapped surface waves or hybrid modes are not considered in this comparison.

Figure 2d gives the line parameters for partial dielectric filling with reduced dimensions $w = w_o/(\epsilon_{eff})^{1/2}$ and $h = h_o/(\epsilon_{eff})^{1/2}$. This insures that the electrical dimension of the two basic line parameters is the same as the electrical dimension of the air line of Fig. 2a. In order to obtain the same impedance for the partially filled microstrip of Fig. 2d and the air line one reduces the ground plane spacing h_o to h_1 as shown in Fig. 2e such that the characteristic impedance of the air line is reduced to $Z_o/(\epsilon_{eff})^{1/2}$.

We can now state that:

(*i*) The microstrip with dielectric material of Fig. 2d and the microstrip without dielectric material of Fig. 2e have the same impedance.

(*ii*) If we assume that the current distribution is uniform for the air line over the width w_o on the ground plane and the adjacent bottom face of the strip we obtain the same unloaded Q for both lines of Fig. 2d and Fig. 2e. The attenuation of the air line is lower by a factor $(\epsilon_{eff})^{1/2}$ as given in Fig. 2e.

IV. COMPUTATION OF LINE PARAMETERS

4.1 *Exact Analytic Solution for Impedance by Conformal Mapping*

The charactreistic impedance of the microstrip of Fig. 2a with thickness $t = 0$ can be obtained by Schwarz-Christoffel integrals which transform the upper half of a complex z_1 plane into a rectangle

in the complex z plane.[8–10] More specifically, one has to find an analytic function which maps the two strip boundaries in the z_1-plane on two opposite sides of the rectangle as shown in Fig. 3. The Schwarz-Christoffel integral for this specific case can be expressed in terms of the theta function ϑ_1 and ϑ_4. Theta functions are well behaved analytic functions of a complex variable, their properties are well known, and rapidly converging series have been published.[11,12] These functions and their logarithmic derivatives are essential mathematical tools for solving the following engineering problems:

(*i*) characteristic impedance of conductors with strip geometries,

(*ii*) junction capacitance in semiconductor diodes with strip junctions,

(*iii*) heat flow and thermal resistance from a line source into a solid, and

(*iv*) series resistance of bulk devices with stripe contacts.

The conformal transformation $z_1 = z_1(z)$ expressed in terms of the logarithmic derivative of the theta function ϑ_1 and its parameter $\kappa =$

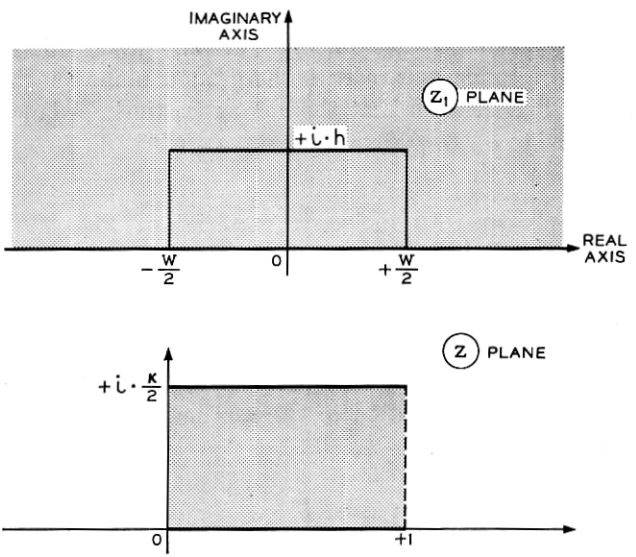

Fig. 3 — Conformal mapping of a microstrip by the logarithmic derivative of the theta function $\vartheta_1(z, \kappa)$.

$$z_1 = -\frac{2hK}{\pi} \frac{\partial \ln \vartheta_1(z, \kappa)}{\partial z}, \quad Z_0 = \left(\frac{\mu_0}{\epsilon_0}\right)^{\frac{1}{2}} \cdot \frac{\kappa}{2}$$

K'/K is

$$z_1 = -\frac{2hK}{\pi}\frac{\partial}{\partial z}\ln \vartheta_1(z, \kappa) \tag{7}$$

where $K = K(m)$ and $K' = K'(m)$ are complete elliptic integrals of the first kind with modulus m.

The characteristic impedance Z_0 of the microstrip with width w, height h, and thickness $t = 0$ is obtained by solving the following equations

$$\frac{w}{h} = \frac{2}{\pi}\frac{\partial}{\partial \zeta}\ln \vartheta_4(\zeta, \kappa) \tag{8}$$

$$\mathrm{dn}^2(2K\zeta) = \frac{E}{K} \tag{9}$$

$$Z_0 = \frac{1}{2}\left(\frac{\mu_0}{\epsilon_0}\right)^{\frac{1}{2}}\frac{K'}{K}. \tag{10}$$

$E = E(m)$ is the complete elliptic integral of the second kind, dn the Jacobian elliptic function, μ_0 and ϵ_0 the magnetic and dielectric permeabilities of free space. With $(\mu_0/\epsilon_0)^{1/2} = 120\pi$ ohm and $\kappa = K'/K$ one obtains

$$Z_0 = 60\pi\kappa \text{ ohm}. \tag{11}$$

For a very narrow strip $w \ll h$ and a very wide strip $w \gg h$ one obtains the simple expressions

$$Z_0 = 60 \ln \frac{8h}{w} \text{ ohm} \qquad w \ll h \tag{12}$$

$$Z_0 = \frac{120\pi h}{w} \text{ ohm} \qquad w \gg h. \tag{13}$$

The exact computation for one important intermediate case by means of a series expansion for the logarithmic derivative of the theta function ϑ_4 is treated in the appendix.

4.2 *Impedance Design Formulas*

The rigorous solution for computing Z_0 from equations (8), (9), and (10) is not recommended for most engineering applications. Useful expressions in terms of rational functions or series expansions can be obtained by generalization of equations (12) and (13) as follows

$$Z_0 = 60 \ln \sum_{n=1}^{-\infty} a_n \left(\frac{h}{w}\right)^n \text{ ohm} \qquad w \leqq h \tag{14}$$

$$Z_o = \frac{120\pi}{\sum_{n=1}^{-\infty} b_n \left(\frac{w}{h}\right)^n} \text{ ohm} \qquad w \geqq h. \tag{15}$$

The number of terms after which the series is terminated determines the accuracy of the approximations. The following formulas obtained by rational function approximation give an accuracy of ± 0.25 per cent for $0 \leqq w/h \leqq 10$ which is the range of importance for most engineering applications

$$Z_o = 60 \ln \left(\frac{8h}{w} + \frac{w}{4h}\right) \text{ ohm} \qquad \frac{w}{h} \leqq 1 \tag{16}$$

$$Z_o = \frac{120\pi \text{ ohm}}{\frac{w}{h} + 2.42 - 0.44\frac{h}{w} + \left(1 - \frac{h}{w}\right)^6} \qquad \frac{w}{h} \geqq 1. \tag{17}$$

The accuracy obtained for strips with $w/h > 10$ from equation (17) is ± 1 per cent.

Table I compares the impedance obtained with theta functions, the impedance calculated from the rational function approximations, and the measured value, with a time domain reflectometer for $w/h = 1$. The physical dimensions of the line used for the time domain reflectometer measurement are listed in Table II.

The estimated maximum error for Z_o is ± 0.7 percent. Measurements for different ratios w/h by the same procedure have also given excellent agreement with data obtained by means of the logarithmic derivative of the theta function $\vartheta_4(\zeta, \kappa)$.

Figure 4 is a plot of Z_o as a function of w/h. The impedance for the important case of the standard microstrip of Fig. 1a is also plotted for two materials which look attractive for hybrid integrated circuits in the microwave and the millimeter wave range. These materials are

TABLE I — CHARACTERISTIC IMPEDANCE FOR $w/h = 1$

Method	Z_o Ohm
Rigorous solution with theta functions eqs. (8), (9), (10)	126.553
Measured impedance with time domain reflectometer (Table II)	126.60
Approximation with narrow strip rational function equation (16)	126.613
Approximation with wide strip rational function equation (17)	126.507

TABLE II — IMPEDANCE MEASUREMENT DATA WITH TIME DOMAIN REFLECTOMETER

Impedance standard, General Radio coaxial precision air line	GR 900-L 50 Ω
Time domain reflectometer, Hewlett Packard	hp 1415A
Microstrip ground plane spacing h,	0.750 inch
width w,	0.750 inch
thickness t	0.001 inch
Dielectric constant of polyfoam support and polyfoam cover	$\epsilon_r = 1.032$
Measured impedance for thickness $t = 0.001$ inches, dielectric constant $\epsilon_r = 1.032$	124.42 Ω
Extrapolated impedance Z for thickness $t = 0$ from measurements for $t = 0.001$ inch, 0.0115 inch, 0.0265 inch, 0.0525 inch and 0.0625 inch	124.62 Ω
Microstrip air line impedance $Z_0 = (\epsilon_r)^{\frac{1}{2}}Z$	126.60 Ω

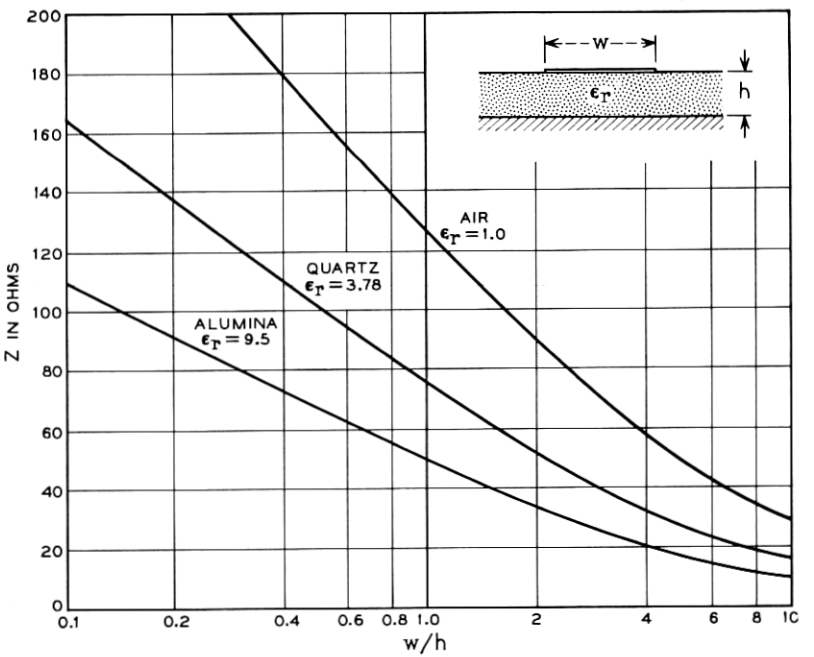

Fig. 4 — Characteristic impedance of the standard microstrip for $\epsilon_r = 1$ and impedance of the standard microstrip for $\epsilon_r = 3.78$ (quartz) and $\epsilon_r = 9.5$ (alumina) as a function of w/h.

fused quartz (SiO_2) with $\epsilon_r = 3.78$ and 99.5 percent alumina (Al_2O_3) with $\epsilon_r = 9.5$ whose impedance curves are based on computed effective dielectric constants treated in Section 4.3.

4.3 *Computation and Measurement of Effective Dielectric Constant*

The electrical parameters of any microstrip can be computed if the characteristic impedance Z_0 of the corresponding air line and the dielectric constant $(\epsilon_{eff})^{1/2}$ are known. The basic equations required for this computation are listed in Fig. 2.

The effective dielectric constant ϵ_{eff} is a function of the ratio w/h, the relative dielectric constant ϵ_r, and the geometrical shape of the boundary between air and the dielectric support material. The effective dielectric constant can be obtained by starting from the transformation given by equation (7), by mapping the boundaries between air and dielectric into the rectangle in the z-plane of Fig. 3, and by treating the new geometrical configuration obtained inside the rectangle of the z-plane as a parallel plate capacitor which is partially filled with dielectric.

Notice that the fringe field problem is eliminated in the z-plane because the complete upper half of the plane is transformed into one rectangle. The procedure is rigorous since conformal mapping preserves the angle of refraction of electric field lines at the boundary between dielectric and air. If the capacitance of the parallel plate configuration in the z-plane of Fig. 3 is C_0 without dielectric and C with partial dielectric filling one obtains

$$\epsilon_{eff} = \frac{C}{C_0}. \tag{18}$$

The method which is outlined above has been used by Wheeler for the standard microstrip of Fig. 1a by starting from an approximate conformal mapping transformation and by using an approximation for the transformed parallel plate capacitance.[13] The square root of the effective dielectric constant $(\epsilon_{eff})^{1/2}$ obtained by this method is shown in Fig. 5 as a function of w/h and ϵ_r.

In order to find a function which approximates the set of curves of Fig. 5 over the total range $0 \leqq w/h < \infty$ and $1 \leqq \epsilon_r < \infty$ we define a function $F(\epsilon_r, w/h)$ by

$$\epsilon_{eff} = \frac{\epsilon_r + 1}{2} + \frac{\epsilon_r - 1}{2} F\left(\epsilon_r, \frac{w}{h}\right). \tag{19}$$

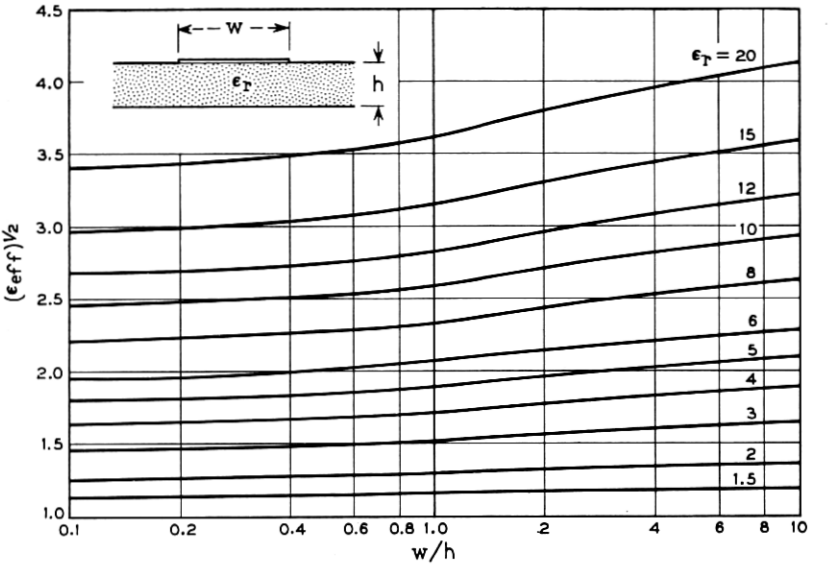

Fig. 5 — Square root of the effective dielectric constant for the standard microstrip. $(\epsilon_{eff})^{1/2}$ plotted as a function of w/h with ϵ_r as parameter.

From equation (5) we find for the standard microstrip of Fig. 1(a)

$$0 \leqq F\left(\epsilon_r, \frac{w}{h}\right) \leqq 1. \tag{20}$$

One class of functions which fulfills this requirement is the class of irrational functions

$$F\left(\epsilon_r, \frac{w}{h}\right) = \left[1 + \sum_{n=1}^{N} c_n \left(\frac{h}{w}\right)^n\right]^m \tag{21}$$

with c_n being functions of ϵ_r and $m \leqq 0$. The set of curves of Fig. 5 can be approximated with $m = -0.5$ and one single term of the series by

$$F\left(\epsilon_r, \frac{w}{h}\right) = \left(1 + \frac{10h}{w}\right)^{-\frac{1}{2}}. \tag{22}$$

The final result with an accuracy of ± 2 per cent for ϵ_{eff} and an accuracy of ± 1 per cent for $(\epsilon_{eff})^{\frac{1}{2}}$ is

$$\epsilon_{eff} = \frac{\epsilon_r + 1}{2} + \frac{\epsilon_r - 1}{2}\left(1 + \frac{10h}{w}\right)^{-\frac{1}{2}}. \tag{23}$$

Effective dielectric constants can also be obtained by static capacitance measurements or time domain reflectometer measurements. If the static capacitance per unit length is C with partial dielectric filling and C_o with the dielectric removed, one obtains $\epsilon_{eff} = C/C_o$ and from $Z = (L/C)^{1/2}$ with $L = Z_o/v_o$

$$Z = \frac{Z_o}{(\epsilon_{eff})^{\frac{1}{2}}} = \frac{1}{v_o(CC_o)^{\frac{1}{2}}} \tag{24}$$

where v_o is the velocity of light in vacuum, $v_o = 3.10^{10}$ cm per second.

Accurate measurements of ϵ_{eff} with a time domain reflectometer require a precision coaxial connector standard and a good transition from coaxial transmission line into the microstrip. Baseband transitions up to a few GHz can be made by building an oversize model of the partially filled microstrip as shown in Fig. 6. The inverted microstrip of Fig. 1(e) used for this measurement is supported by clear fused and polished quartz plates with a dielectric constant $\epsilon_r = 3.78$. The effective dielectric constant ϵ_{eff} plotted as a function of w/h is much lower than ϵ_r because only a small fraction of field lines passes through the quartz. Similar results are obtained if the line shown in Fig. 6 is completely shielded provided that the major part of the radio frequency energy remains concentrated in the

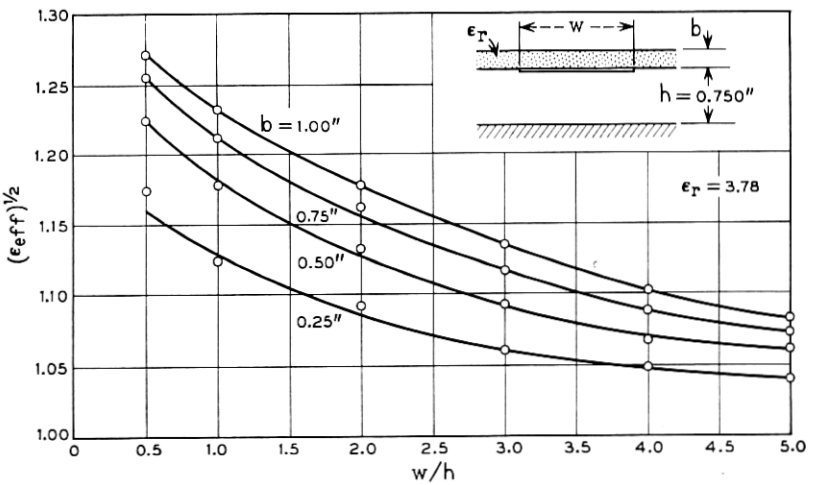

Fig. 6 — Square root of the effective dielectric constant for an inverted microstrip with quartz substrate. Oversize measurement with strip conductor thickness $t = 0.010$ inch.

air gap between the ground plane and the strip conductor. One concludes from this measurement that all of the electrical parameters of inverted microstrips are close to the electrical parameters of the air line. One also concludes that dielectric losses are substantially reduced because all the dielectric support material is removed into the low field region of the microstrip.

4.4 *Computation of Conductor Attenuation*

The attenuation of any lumped or distributed circuit element is known if its inductance as a function of the geometrical conductor parameters can be calculated. Inductance and conductor attenuation are related because the inductance is the normalized magnetic field energy of the circuit element and attenuation is proportional to the magnetic field energy stored in the metal conductor.[14] In order to calculate the attenuation one has to recede the metal surface by one skin depth or more generally by a small length δn normal to the conductor surface. If the corresponding increase in inductance is δL and if the skin resistance of the metal is R_s, then the radio frequency resistance R of the circuit or line element is

$$R = \frac{R_s}{\mu_o}\frac{\delta L}{\delta n} \tag{25}$$

with the skin resistance R_s given by

$$R_s = (\pi \mu_o f \rho)^{\frac{1}{2}} \text{ ohm} \tag{26}$$

where f is the frequency in Hz, ρ the conductor resistivity in ohm·cm, and $\mu_o = 4\pi \cdot 10^{-9}$ henry per cm. The skin resistance in ohms as a function of frequency is plotted in Fig. 7 with ρ in ohm·cm as a parameter.

The inductance L and the attenuation α_o in neper per unit length of a microstrip which supports a transverse electromagnetic mode are given by

$$L = (\epsilon_o \mu_o)^{\frac{1}{2}} Z_o \tag{27}$$

$$\alpha_o = \frac{R}{2Z_o}. \tag{28}$$

From equations (25), (27), and (28) one obtains

$$\alpha_o = \left(\frac{\epsilon_o}{\mu_o}\right)^{\frac{1}{2}} \frac{R_s}{2Z_o}\frac{\delta Z_o}{\delta n}. \tag{29}$$

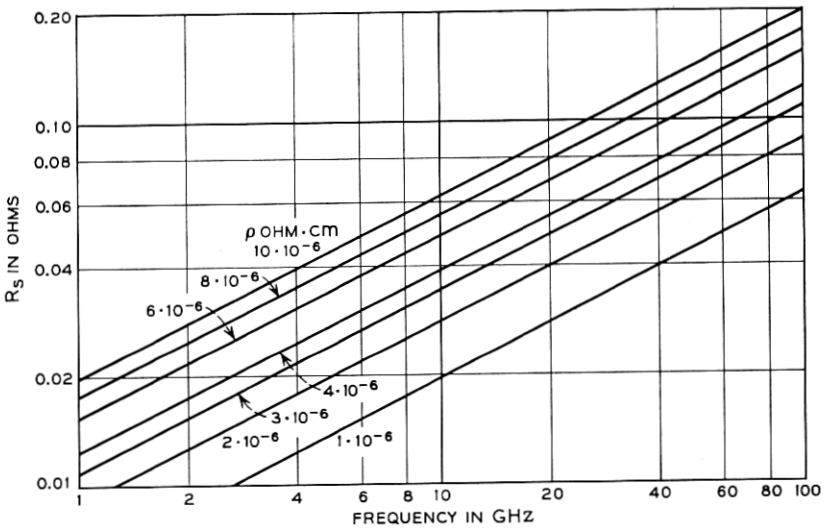

Fig. 7 — Skin resistance R_s of metals as a function of frequency. Bulk resistivity at dc and 20°C for suitable conductors is 1.7 μohm·cm for copper, 1.6 μohm·cm for silver, 2.3 μohm·cm for gold, and 2.8 μohm·cm for aluminum.

The geometrical conductor parameters of the microstrip are width w, height h and thickness t. Let us assume first that the skin resistance of the ground plane is different from the skin resistance of the strip, for example, the two conductor materials are not the same. The attenuation α_1 owing to the ground plane with a skin resistance R_{s1} is obtained by receding the metal surface by $\delta n = \delta h$

$$\alpha_1 = \left(\frac{\epsilon_o}{\mu_o}\right)^{\frac{1}{2}} \frac{R_{s1}}{2Z_o} \frac{\partial Z_o}{\partial h}. \tag{30}$$

The strip attenuation α_2 with a skin resistance R_{s2} is obtained by reducing the strip dimensions by $2\delta w$ and $2\delta t$ as well as increasing the ground plane spacing by δh

$$\alpha_2 = \left(\frac{\epsilon_o}{\mu_o}\right)^{\frac{1}{2}} \frac{R_{s2}}{2Z_o} \left[\frac{\partial Z_o}{\partial h} - 2\frac{\partial Z_o}{\partial w} - 2\frac{\partial Z_o}{\partial t}\right]. \tag{31}$$

The total attenuation α_o is

$$\alpha_o = \alpha_1 + \alpha_2 . \tag{32}$$

If the conductor materials for the ground plane and the strip are the same we obtain with $R_{s1} = R_{s2} = R_s$

$$\alpha_o = \left(\frac{\epsilon_o}{\mu_o}\right)^{\frac{1}{2}} \frac{R_s}{Z_o}\left(\frac{\partial Z_o}{\partial h} - \frac{\partial Z_o}{\partial w} - \frac{\partial Z_o}{\partial t}\right). \tag{33}$$

It is useful to write the partial derivatives:

$$\frac{\partial Z_o}{\partial w} = +\frac{1}{h}\frac{\partial Z_o}{\partial\left(\frac{w}{h}\right)} \tag{34}$$

$$\frac{\partial Z_o}{\partial h} = -\frac{w}{h^2}\frac{\partial Z_o}{\partial\left(\frac{w}{h}\right)} \tag{35}$$

$$\frac{\partial Z_o}{\partial t} = +\frac{\partial Z_o}{\partial w}\frac{\partial w}{\partial t} \tag{36}$$

with $\partial w/\partial t$ being the derivative of w with respect to t for constant Z_o. The attenuation α_o in dB per unit length is finally

$$\alpha_o = -\frac{R_s}{6\pi \ln 10}\frac{\partial Z_o}{\partial\left(\frac{w}{h}\right)}\frac{1 + \frac{w}{h} + \frac{\partial w}{\partial t}}{hZ_o}. \tag{37}$$

The partial derivative $\partial w/\partial t$ can be derived from approximate expressions published by Wheeler, Caulton, Hughes, and Sobol.[13,15] They define an effective width $w_{eff} = w + \Delta w$ by considering two different microstrips with the same characteristic impedance Z_o and different dimensions given by w, h, $t \neq 0$ and w_{eff}, h, $t = 0$. The approximations are

$$\Delta w = w_{eff} - w = \frac{t}{\pi}\left(1 + \ln\frac{4\pi w}{t}\right) \qquad \frac{w}{h} \leqq \frac{1}{2\pi} \tag{38}$$

$$\Delta w = w_{eff} - w = \frac{t}{\pi}\left(1 + \ln\frac{2h}{t}\right) \qquad \frac{w}{h} \geqq \frac{1}{2\pi}. \tag{39}$$

Additional restrictions for applying equations (38) and (39) are $t \ll h$, $t < w/2$, and $t/\Delta w < 0.75$. Notice also that the ratio $\Delta w/t$ obtained from equations (38) or (39) is divergent for $t \to 0$. This does not present a problem since equations (29) to (37) are only applicable if the conductor thickness exceeds several skin depths.

Being aware of these limitations, we obtain the partial derivatives $\partial w/\partial t$ by computing $\partial w_{eff}/\partial t$ from equations (38) and (39)

$$\frac{\partial w}{\partial t} = \frac{1}{\pi}\ln\frac{4\pi w}{t} \qquad \frac{w}{h} \leqq \frac{1}{2\pi} \tag{40}$$

$$\frac{\partial w}{\partial t} = \frac{1}{\pi} \ln \frac{2h}{t} \qquad \frac{w}{h} \geqq \frac{1}{2\pi}. \tag{41}$$

It is convenient for design purposes to define the normalized attenuation A in dB per ohm as follows

$$A = \frac{h\alpha_o}{R_s} = -\frac{1}{6\pi \ln 10} \frac{\partial Z_o}{\partial\left(\frac{w}{h}\right)} \frac{1 + \frac{w}{h} + \frac{\partial w}{\partial t}}{Z_o}. \tag{42}$$

A is plotted in Fig. 8 as a function of w/h with $\partial w/\partial t$ as a parameter. The normalized attenuation A based on the assumption of uniform current distribution over the width w of the bottom conductor and the adjacent bottom side of the strip conductor is also shown in Fig. 8 for comparison. The formula valid for uniform current distribution is

$$A = \frac{20}{\ln 10} \frac{h}{wZ_o} \frac{\text{dB}}{\text{ohm}}. \tag{43}$$

One can show that equations (42) and (43) give the same result for $w/h \gg 1$ since $Z_o = 120\pi h/w$ and $\partial Z_o/\partial(w/h) = -120\pi h^2/w^2$. This is expected because fringe fields can be neglected for wide strips. One obtains a lower attenuation from equation (42) for narrow strips because currents are flowing on the top and bottom side of the strip and also because of the beneficial effect of wider current distribution in the ground plane because of fringe fields. For narrow strips the result is with $Z_o = 60 \ln (8h/w + w/4h)$ ohm

$$A = \frac{10}{\pi \ln 10} \frac{\left(\frac{8h}{w} - \frac{w}{4h}\right)\left(1 + \frac{h}{w} + \frac{h}{w}\frac{\partial w}{\partial t}\right)}{Z_o \exp\left(\frac{Z_o}{60}\right)} \qquad \frac{w}{h} \leqq 1. \tag{44}$$

For wide strips one obtains from equations (17) and (42)

$$A = \frac{Z_o}{720\pi^2 \ln 10}\left[1 + \frac{0.44h^2}{w^2} + \frac{6h^2}{w^2}\left(1 - \frac{h}{w}\right)^5\right]\left(1 + \frac{w}{h} + \frac{\partial w}{\partial t}\right)$$

$$\frac{w}{h} \geqq 1. \tag{45}$$

For design purposes it is recommended to read R_s and A from Figs. 7 and 8 and to obtain α_o in dB per unit length from

$$\alpha_o = \frac{R_s A}{h}. \tag{46}$$

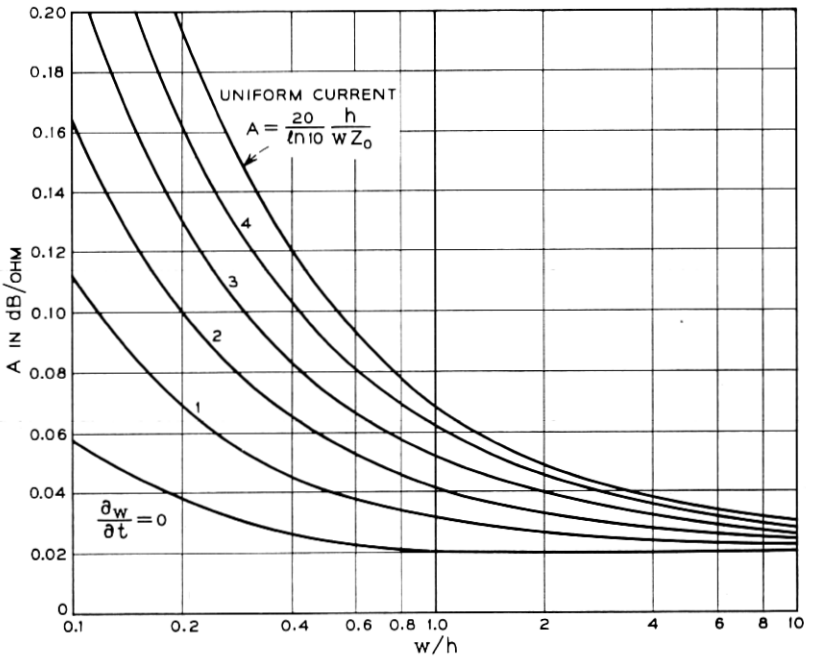

Fig. 8 — Normalized conductor attenuation $A = \alpha_0 h/R_s$ in dB per ohm for a standard microstrip with $\epsilon_r = 1$. The partial derivative $\partial w/\partial t$ is a function of the conductor thickness t and given by equations (40) and (41). The conductor attenuation for partial dielectric filling is $\alpha = (\epsilon_{eff})^{1/2} \alpha_0$ as given by equation (3).

The conductor attenuation for partial dielectric filling is obtained from equation (3).

4.5 *Measurement of Microstrip Attenuation*

Measurements of the microstrip attenuation in the 1 to 6 GHz frequency range have been performed by Caulton, Hughes, Sobol, Pucel, Massé, and Hartwig.[15,16] Good agreement between theory and experiment has been obtained in Ref. 15 based on the assumption of uniform current distribution. Good agreement is also obtained in Ref. 16 based on the assumption of the correct nonuniform current distribution. This can be explained in part because the skin resistance R_s used for the calculations in Ref. 16 is based on the dc resistivity of the copper conductor plus a sizable correction in order to account for surface roughness. This correction increases R_s by 13 percent at 1 GHz and 33 percent at 6 GHz. From recent work by L. U. Kibler

one concludes that this correction may be too large even if one takes into account the fact that the data obtained by Kibler in Ref. 17 are based on electroformed oxygen free copper without any additional treatment for improving the surface finish.

The measurement of attenuation at 30 GHz requires a low loss transition from waveguide into microstrip. Such a transition has been developed by W. F. Bodtmann.[18] Clear fused and polished quartz substrates are used for the substrate material in order to obtain a low effective dielectric constant. Evaporated and photoetched nichrome-gold layers with a thickness of 2 μm are used for the conductor materials on both substrate surfaces. Table III summarizes the properties of the microstrip.

Table IV gives the attenuation measured for a 3-inch long microstrip line by means of a transmission measurement with two-waveguide to microstrip transition at both ends of the microstrip. The theoretical loss based on the assumption of uniform current distribution and the theoretically computed current distribution is given in Table V.

The agreement between measured and calculated data does not necessarily support the uniform current theory. It indicates as expected that the radio frequency film resistivity ρ at 30 GHz is higher than the dc resistance of Table V. The dc resistivity is calculated from a measurement of the composite nichrome-gold resistance and a thickness measurement with a Tolansky interferometer.

The attenuation α' per guide wavelength is 0.0609 dB. A value from 0.060 to 0.068 dB has been measured in the 26.5 to 30.5 GHz frequency range. The unloaded Q is given by

$$Q = \frac{20\,\pi}{\ln 10}\,\frac{1}{\alpha_o \lambda_o} = \frac{27.3}{\alpha'} = 450. \tag{47}$$

TABLE III — MICROSTRIP DATA

Type of microstrip	standard of Fig. 1a
Substrate material*	clear fused quartz
Substrate thickness h	0.030 inch
Conductor width w	0.030 inch
Conductor thickness t	2 μm Nichrone-gold
Metal deposition	evaporated
Thickness of Nichrome base layer	100 to 150 A
Line fabrication	photoetching
Conductor resistivity	$\rho = 3.0 \cdot 10^{-6}$ Ohm·cm

* 99.8 percent SiO_2, Amersil Inc., Hillside, New Jersey.

TABLE IV—MEASURED MICROSTRIP LOSS AT 30 GHz

Measured total loss of waveguide to microstrip transitions and 3-inch long microstrip at 30 GHz	0.88 dB
Measured insertion loss for both transitions (two transitions back to back)	0.10 dB
Attenuation for line length l = 3 inches	0.78 dB

This is believed to be the highest Q obtained for a microstrip in this frequency range.

V. MODE PROPAGATION IN MICROSTRIPS

Microstrip transmission lines which are fully shielded and completely filled with dielectric material can propagate transverse electromagnetic, transverse electric, and transverse magnetic modes. Partially filled and fully shielded lines cannot support these modes because the boundary conditions at the interface between air and dielectric cannot be rigorously fulfilled. Zysman and Varon have shown that a hybrid mode can be found which satisfies all boundary conditions and which can be decomposed into sums of transverse electric and transverse magnetic space harmonics.[19] From their results one concludes that the hybrid mode propagates at all frequencies and that it approaches the transverse electromagnetic mode at low frequencies or for sufficiently small line dimensions.

The problem of hybrid mode propagation has also been treated by Pregla, Schlosser, Hartwig, Massé, and Pucel.[20,21] One concludes from the results that the frequency dependent behavior or the dispersion of the propagation constant and the effective dielectric constant is

TABLE V—THEORETICAL MICROSTRIP LOSS AT 30 GHz

Square root of effective dielectric constant for $\epsilon_r = 3.78$ and $w/h = 1$, equation (23)	$(\epsilon_{eff})^{\frac{1}{2}} = 1.68$
Conductor skin resistance for f = 30 GHz and $\rho = 3.0 \times 10^{-6}$ ohm·cm, Fig. 7	$R_s = 0.060$ ohm
Normalized attenuation, uniform current distribution, $w/h = 1$, Fig. 8	$A = 0.0685$ dB per ohm
Normalized attenuation, nonuniform current distribution, $\partial w/\partial t = 2.1$, Fig. 8	$A = 0.0420$ dB per ohm
Attenuation, line length $l = 3''$, $(\epsilon_{eff})^{\frac{1}{2}} R_s A l/h$, uniform current	0.690 dB
Attenuation, line length $l = 3''$ Nonuniform current distribution	0.423 dB

particularly pronounced for lines with substrates which have a high dielectric constant, such as alumina with $\epsilon_r = 9.6$ and rutile with $\epsilon_r = 104$. It is also shown that the frequency of operation has to be lower than the cutoff frequency f_c of the lowest order transverse electric surface wave which is given by

$$f_c = \frac{75}{h(\epsilon_r - 1)^{\frac{1}{2}}} \text{ GHz} \tag{48}$$

where h is the substrate thickness in millimeter.[21] The cutoff frequency obtained for the line of Table III with $h = 0.75$ mm and $\epsilon_r = 3.78$ is $f_c = 60$ GHz. For high density alumina with $\epsilon_r = 9.6$ the cutoff is considerably lower with $f_c = 34$ GHz.

VI. CONCLUSIONS

The electrical properties of microstrips can be derived from the characteristic impedance of the air line and the effective dielectric constant if the propagating mode can be approximated by a transverse electromagnetic mode. Substrates with a low dielectric constant are useful for circuit applications because dispersion of the line parameters is less pronounced. Structures with an air gap are recommended if circuit losses have to be minimized. Complete shielding is essential for most applications in order to reduce radiation loss and to reduce the coupling between different circuits.

VII. ACKNOWLEDGMENT

The author expresses his thanks to S. Michael and W. W. Snell for performing exact measurements and to S. Shah for providing high quality films.

APPENDIX

Computing Microstrip Impedance with Theta Functions

The following example gives the numerical procedure for computing the characteristic impedance of a microstrip. It is convenient to calculate w/h and Z_0 as a function of the modulus m of the complete elliptic integrals K, K', and E. We assume $m = 0.86$ for this example and use equations (8), (9), and (10)

(*i*) $m = 0.86$ modulus of complete elliptic integrals

(*ii*) $K = 2.42093$
$K' = 1.63058$
$E = 1.13600$
$\kappa = K'/K = 0.673532.$
} From tables, Ref. 22.

(*iii*) Characteristic impedance from equation (10) with $(\mu_o/\epsilon_o)^{\frac{1}{2}} = 120\pi$ ohm

$$Z_o = 60\pi \frac{K'}{K} = 126.958 \text{ ohm}. \tag{49}$$

(*iv*) From equation (9) and tables of the Jacobian elliptic functions we obtain[23]

$$\mathrm{dn}^2(2K\zeta) = \frac{E}{K} = 0.469240 \tag{50}$$

$$2K\zeta = \mathrm{arc\,dn}\left(\frac{E}{K}\right)^{\frac{1}{2}} = 1.02806 \tag{51}$$

$$\zeta = 0.212328. \tag{52}$$

(*v*) We use the rapidly converging series expansion[12]

$$\frac{\partial}{\partial \zeta} \ln \vartheta_4(\zeta, \kappa) = 4\pi \sum_{n=1}^{\infty} \frac{\exp(-n\pi\kappa)}{1 - \exp(-2n\pi\kappa)} \sin(2n\pi\zeta) \tag{53}$$

and obtain for the sum S of the first 10 terms $S = 0.124095$.

(*vi*) From equation (10) we obtain

$$\frac{w}{h} = \frac{2}{\pi} \frac{\partial}{\partial \zeta} \ln \vartheta_4(\zeta, \kappa) = 0.992762. \tag{54}$$

The result listed in Table I is based on quadratic interpolation from a table made with closely spaced moduli m.

REFERENCES

1. Ruthroff, C. L., Osborne, T. L., and Bodtmann, W. F., "Short Hop Radio System Experiment," scheduled for B.S.T.J., *48*, No. 6 (July–August 1969).
2. Tillotson, L. C., "A Model of a Domestic Satellite Communication System," B.S.T.J., *47*, No. 10 (December 1968), pp. 2111–2137.
3. Brenner, H. E., "Use a Computer to Design Suspended-Substrate Integrated Circuits," Microwaves, *7*, No. 9 (September 1968), pp. 38–45.
4. Engelbrecht, R. S., and Kurokawa, K., "A Wideband Low Noise L-Band Balanced Transistor Amplifier," Proc. IEEE, *53*, No. 3 (March 1965), pp. 328–333.
5. Saunders, T. E., and Stark, P. D., "An Integrated 4-GHz Balanced Transistor Amplifier," IEEE J. Solid State Elec., *SC-2*, No. 1 (March 1967), pp. 4–10.
6. Bonfeld, M. D., Bonomi, M. J., and Jaasma, E. G., "An Integrated Micro-

wave FM Discriminator," 1968 G-MTT Int. Microwave Symp. Digest, Detroit, Michigan, May 20–22, 1968, pp. 139–146.
7. Cohn, S. B., "Slot Line—An Alternative Transmission Medium for Integrated Circuits," 1968 G-MTT Int. Microwave Symp. Digest, Detroit, Michigan, May 20–22, 1968, pp. 104–109.
8. Binns, K. J., and Lawrenson, P. J., *Electric and Magnetic Field Problems,* New York: MacMillan, 1963, pp. 157–224.
9. Moon, P., and Spencer, D. E., *Field Theory for Engineers,* New York: D. Van Nostrand, 1961, pp. 339–357.
10. Smythe, W. R., *Static and Dynamic Electricity,* New York: McGraw Hill, 1950, pp. 82–101.
11. Bellman, R., *A Brief Introduction to Theta Functions,* New York: Holt Rinehart and Winston, 1961, pp. 1-72.
12. Tölke, F., *Praktische Funktionenlehre, Zweiter Band, Theta-Funktionen und Spezielle Weierstrass' sche Funktionen,* Berlin: Springer Verlag, 1966, pp. 1–83.
13. Wheeler, H. A., "Transmission-Line Properties of Parallel Strips Separated by a Dielectric Sheet," IEEE Trans. Microwave Theory and Techniques, *MTT-13,* No. 2 (March 1965), pp. 172–185.
14. Wheeler, H. A., "Formulas for the Skin Effect," Proc. IRE, *30,* No. 9 (September 1942), pp. 412–424.
15. Caulton, M., Hughes, J. J., and Sobol, H., "Measurement of the Properties of Microstrip Transmission Lines for Microwave Integrated Circuits," RCA Review, *27,* No. 3 (September 1966), pp. 377–391.
16. Pucel, R. A., Massé, D. J., and Hartwig, C. P., "Losses in Microstrip," IEEE Trans. Microwave Theory and Techniques, *MTT-16,* No. 6 (June 1968), pp. 342–350.
17. Kibler, L. U., "The Properties and Uses of the Cutoff Frequency Region of a Lossy Rectangular Waveguide," Ph.D. Thesis, Polytechnic Institute of Brooklyn, June 1968.
18. Schneider, M. V., Glance, B., and Bodtmann, W. F., "Microwave and Millimeter Wave Hybrid Integrated Circuits for Radio Systems," scheduled for B.S.T.J., *48,* No. 6 (July–August 1969).
19. Zysman, G. I., and Varon, D., "Wave Propagation in Microstrip Transmission Lines," Int. Microwave Symp., IEEE Group on Microwave Theory and Techniques, Dallas, Texas, May 5–7, 1969.
20. Pregla, R., and Schlosser, W., "Waveguide Modes in Dielectrically Supported Strip Lines," Archiv der Elektrischen Uebertragung, *22,* No. 8 (August 1968), pp. 379–386.
21. Hartwig, C. P., Massé, D., and Pucel, A. P., "Frequency Dependent Behavior of Microstrip," 1968 G-MTT Int. Microwave Symp. Digest, Detroit, Michigan, May 20–22, 1968, pp. 110–116.
22. Abramowitz, M., and Stegun, I. A., *Handbook of Mathematical Functions,* National Bureau of Standards, Applied Mathematics Series 55, 2nd printing, November 1964, pp. 608–609.
23. Fettis, H. E., and Caslin, J. C., *Ten Place Tables of the Jacobian Elliptic Functions,* Aerospace Research Laboratories, Wright Paterson Air Force Base, Ohio, AD 631–869, September 1965.